A Complementary Modularized Ramp Metering Approach Based on Iterative Learning Control and ALINEA

Zhongsheng Hou, Xin Xu, Jingwen Yan, Jian-Xin Xu, *Senior Member, IEEE*, and Gang Xiong

***Abstract*—Ramp metering is an effective tool for traffic management on freeway networks. In this paper, we apply iterative learning control (ILC) to address ramp metering in a macroscopic-level freeway environment. By formulating the original ramp metering problem as an output regulating and disturbance rejection problem, ILC has been applied to control the traffic response. The learning mechanism is further combined with Asservissement Linéaire d'Entrée Autoroutière (ALINEA) in a complementary manner to achieve the desired control performance. The ILC-based ramp metering strategy and the modified modularized ramp metering approach based on ILC and ALINEA in the presence of input constraints are also analyzed to highlight the advantages and the robustness of the proposed methods. Extensive simulations are given to verify the effectiveness of the proposed approaches.**

***Index Terms*—ALINEA, iterative learning control (ILC), ramp metering, traffic control.**

I. Introduction

AN INCREASINGLY important area in the field of intelligent transportation systems is freeway traffic control, which has become feasible owing to the freeway infrastructure development in metropolitan areas in both developed and developing countries. Ramp metering, when properly applied, is an effective tool for efficient traffic management on freeways and freeway networks [1]. The purpose of ramp metering is to regulate the amount of traffic entering a given freeway at its entry ramps so that the freeway can operate at a desired level of service. Ramp metering is useful when traffic is not in an extreme situation. Ramp metering will not be needed if the traffic is too light and be ineffective if the traffic is too dense because breakdown will happen anyway. Ramp metering is implemented by placing a traffic light at the on-ramp that allows the vehicles to enter the freeway in a controlled way and thus reduces the disturbance of the traffic on the mainline. From the viewpoint of the administrative agent of a freeway, an appropriate control mechanism is needed so that incoming traffic does not lead to overflow or underflow on the freeway. By overflow, the freeway is overly utilized and accidents or congestion may easily occur. By underflow, a low utilization rate of the freeway incurs, and it is not cost effective. Thus, the objective of ramp metering is to maintain a desired level of service for the freeway system such that the freeway system can efficiently be utilized.

Ramp metering strategies can be classified into two categories [1]. One category is the reactive strategy aiming at maintaining the freeway traffic conditions close to the desired values by means of real-time measurements. The other is the proactive strategy aiming at specifying optimal traffic conditions for a whole freeway or freeway network based on demands and model predictions over a sufficiently long time horizon. Reactive ramp metering may be local or coordinated. Local strategies make use of traffic measurements in the vicinity of each ramp, calculating the corresponding individual ramp metering values, whereas coordinate strategies use available traffic measurements from a larger portion of a freeway. Local strategies are far easier to design and implement. Nevertheless, they have been proven to be noninferior to more sophisticated coordinated approaches under recurrent traffic congestion conditions [2].

The most well-known local ramp metering strategies are the demand–capacity (DC) strategy [3], the occupancy (OCC) strategy [3], and ALINEA [4]. The DC and OCC strategies are feedforward schemes because they use upstream measurements. However, the upstream states could be affected by on-ramps during congestion. ALINEA is a feedback regulator that is based on mainstream measurements of occupancy downstream of the ramp. ALINEA has been found to lead to significantly better performance as compared with DC and OCC strategies in several comparative field evaluations [2]. According to a recent report, ALINEA has been implemented in various sites in five European countries [5]. Some advanced control methods, such as fuzzy logic control [6] and neural networks (NNs) [7], which have good learning mechanisms to fit particular traffic patterns, are also proposed for local ramp

Manuscript received November 21, 2010; revised February 24, 2011; accepted May 5, 2011. Date of publication June 20, 2011; date of current version December 5, 2011. This work was supported in part by the National Science Foundation of China under Grant 60834001, by the State Key Laboratory of Rail Traffic Control and Safety of Beijing Jiaotong University under Grant RCS2009ZT011, and by the Program for Changjiang Scholars and Innovative Research Team in University under Grant IRT0949. The Associate Editor for this paper was L. Li.

Z. Hou and J. Yan are with the Advanced Control Systems Laboratory, School of Electronic and Information Engineering, Beijing Jiaotong University, Beijing 100044, China (e-mail: zhshhou@bjtu.edu.cn).

X. Xu is with the Institute of Automation, College of Mechatronics and Automation, National University of Defense Technology, Changsha 410073, China (e-mail: xinxu@nudt.edu.cn).

J.-X. Xu is with the Department of Electrical and Computer Engineering, National University of Singapore, Singapore 119260 (e-mail: elexujx@nus.edu.sg).

G. Xiong is with the Automation Institute, Chinese Academy of Science, Beijing 100080, China (e-mail: gangxiong@hotmail.com).

Digital Object Identifier 10.1109/TITS.2011.2157969

metering. However, these methods are not so easy to implement in practice due to their rather complicated controller structures.

Traffic flow patterns are in general repeated every day. For instance, the traffic flow will start from a very low level at midnight and gradually increase up to the first peak of morning rush hour, which is often from 7 to 9 A.M., and the second peak from 5 to 7 P.M. Congestion typically starts at the same location every day. Based on this observation, the iterative learning control (ILC)-based ramp metering strategy has been proposed for freeway density control [8], [9] in a daily or weekly basis. In [8], the basic ILC-based ramp metering and speed control are discussed. In [9], the learning mechanism combined with a pure error feedback in a complementary manner is studied, and the simulation results have shown its superiority to pure ILC-based or pure-feedback controllers.

ILC was first proposed in [10] for the control of a system that repeats the same task in a finite interval. Since then, ILC has extensively been studied and achieved significant progresses in both theory and applications [8], [9], [11]–[13]. ILC has a very simple structure, i.e., an integrator along the iteration axis. It requires very little system knowledge; only the bound of the direct transmission term (in general the Jacobian) of the system input/output is needed to guarantee the learning convergence iteratively. Thus, it is almost a model-free method. This is a very desirable feature in traffic control as the traffic model and the environmental factors may not be well known in practice.

The goal of this paper is to design and analyze the ILC-based control laws for the freeway traffic system with day-to-day strict repeatability, which can either work independently or cowork with the existing ALINEA controller, generating a sequence of control input profiles that drive the traffic flow density to the desired level in the presence of modeling uncertainties, unknown disturbances (exogenous quantities that are not measurable), and input constraint.

The main contributions of this paper include the following three points. First, the well-known ALINEA strategy is used instead of the pure error feedback. Second, a new complementary configuration for the feedforward ILC controller and the feedback ALINEA is proposed. Third, the input saturation is studied for the ILC controller alone and for the complementary configuration, respectively.

The main advantages of ILC-based ramp metering strategies over other intelligent control methods, such as fuzzy logic control and NN control, can be summarized here. First, the learning mechanism of ILC is much simpler than other learning mechanisms, hence easy to implement. Second, although simple in structure, the effectiveness of the ILC-based approach, such as learning convergence, is analyzed and guaranteed with mathematical rigor for nonlinear traffic dynamics, whereas the efficacy of other intelligent control methods, such as the fuzzy- or NN-based ramp metering strategies, is only justified through a simulation study or by experimental results on a particular freeway. In the freeway traffic control field, the design of a theory-supported macroscopic controller is an issue that has yet to be addressed. Third, owing to the simplicity, ILC can easily be added to existing feedback controllers, such as ALINEA, with rigorous analysis. Fourth, in ILC design, the prior knowledge or historical information/data required is very minor.

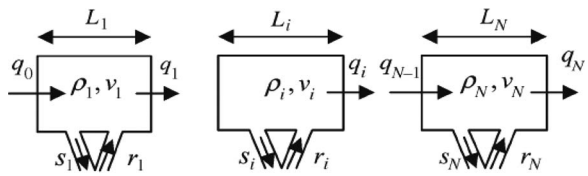

Fig. 1. Segments on a freeway with on/off ramp.

Fuzzy logic control and NN control, on the other hand, would not be easy to implement due to the high complexity and nonlinear structure and the unavailability on the dynamic knowledge or the impractical real-time training data of the freeway traffic. Finally, the convergences for the ILC-based and the modified ILC-based freeway control approaches do not depend on the model parameters and traffic flow model, whereas the time-varying parameters and the uncertainties in the macroscopic model, which are common in a traffic system, will deteriorate the rules and NN-based controller's performance.

This paper is organized as follows: In Section II, the discrete traffic flow model is introduced. In Section III, the convergence analysis of the ILC-based ramp metering and the complementary modularized ramp metering approach based on ILC and ALINEA are presented. The input saturation is studied for the ILC controller alone and for the complementary configuration in Section IV. Case studies with simulations are provided in Section V. Section VI concludes this paper.

II. Traffic Flow Model and Problem Formulation

A. Traffic Flow Model

The analogy between traffic flow and fluid flow forms the basis for the first traffic flow model [14], which is further modified in [15] and [16]. A more sophisticated model, which is proposed in [17]–[19], is tested and validated using real-time traffic data from the Boulevard Peripherique in Paris. In this paper, we will use the model from [17]–[19].

The space and time discretized traffic flow model for a single freeway lane with one on-ramp and one off-ramp is shown in Fig. 1, and its formulation is given as follows:

$$\rho_i(k+1) = \rho_i(k) + \frac{T}{L_i}\left[q_{i-1}(k) - q_i(k) + r_i(k) - s_i(k)\right] \quad (1)$$

$$q_i(k) = \omega\rho_i(k)v_i(k) + (1-\omega)\rho_{i+1}(k)v_{i+1}(k) \quad (2)$$

$$\begin{aligned} v_i(k+1) = {} & v_i(k) + \frac{T}{\tau}\left[V\left(\rho_i(k)\right) - v_i(k)\right] \\ & + \frac{T}{L_i}v_i(k)\left[v_{i-1}(k) - v_i(k)\right] \\ & - \frac{\nu T}{\tau L_i}\frac{\left[\rho_{i+1}(k) - \rho_i(k)\right]}{\left[\rho_i(k) + \kappa\right]} \end{aligned} \quad (3)$$

$$V\left(\rho_i(k)\right) = v_{\text{free}}\left(1 - \left[\frac{\rho_i(k)}{\rho_{\text{jam}}}\right]^l\right)^m \quad (4)$$

where T is the sample time interval in hours, $k = \{0, 1, \ldots, K\}$ is the kth time interval, $i = \{1, 2, \ldots, N\}$ is the ith section of

a freeway, and N is the total number of sections. The model variables are listed as follows:

$\rho_i(k)$	density in section i at time kT (in vehicles per lane per kilometer);
$v_i(k)$	space mean speed in section i at time kT (in kilometers per hour);
$q_i(k)$	traffic flow leaving section i and entering section $i+1$ at time kT (in vehicles per hour);
$r_i(k)$	on-ramp traffic volume for section i at time kT (in vehicles per hour);
$s_i(k)$	off-ramp traffic volume for section i at time kT (in vehicles per hour), which is regarded as an unknown disturbance;
L_i	length of freeway in section i (in kilometers);
v_{free} and ρ_{jam}	free speed and maximum possible density per lane, respectively.

κ, τ, and ν are constant parameters characterizing a given traffic system in terms of the vehicle characteristics, drivers' behaviors, freeway geometry, etc., in units of vehicles per kilometer, hours, and square kilometers per hour, respectively. l, m, and ω are coefficients of the model. For a real-life network, those parameters are determined by a validation procedure. A validated model, however, that is accurate for one place may not hold in another place. The macroscopic model is shown to work fairly accurately with L_i in the order of 500 m or less. For numerical conservation reasons, T and L_i should be chosen such that $T < L_i/v_{\text{free}}$.

Equation (1) is the conservation equation, (2) is the flow equation, (3) is the empirical dynamic speed equation, and (4) represents the density-dependent equilibrium speed.

B. Boundary Conditions

We assume that the traffic flow rate entering section 1 during the time periods kT and $(k+1)T$ is $q_0(k)$, and the mean speed of the traffic entering section 1 is equal to the mean speed of section 1, i.e., $v_0(k) = v_1(k)$. We also assume that the mean speed and the traffic density of the traffic exiting section $N+1$ are equal to those of section N, i.e., $v_{N+1}(k) = v_N(k)$, $\rho_{N+1}(k) = \rho_N(k)$. The boundary conditions can be summarized as follows:

$$\rho_0(k) = q_0(k)/v_1(k) \tag{5}$$

$$v_0(k) = v_1(k) \tag{6}$$

$$\rho_{N+1}(k) = \rho_N(k) \tag{7}$$

$$v_{N+1}(k) = v_N(k) \qquad \forall k. \tag{8}$$

C. Control Objective

Let $\mathbf{I}_p$ denote the set of sections that have on-ramps, i.e., $\mathbf{I}_p = [i_1, i_2, \ldots, i_p]$, where i_j $(j = 1, 2, \ldots, p)$ is the number of the section with an on-ramp, and p is the total number of sections with on-ramps.

$\Re$ is a linear transformation mapping in a normed space $\mathbf{X}^N$, i.e., $\Re : \mathbf{X}^N \to \mathbf{X}^p$, and $\Re(\mathbf{X}) = Q\mathbf{X}$, where $\mathbf{Q} = [\varepsilon_{i_1}, \varepsilon_{i_2}, \ldots, \varepsilon_{i_p}]^T$ is a $p \times N$ matrix, and $\varepsilon_{i_j} = [0, \ldots 0,\ 1,\ 0, \ldots, 0]^T$ represents the unit vector with only the i_jth component to be 1. Further define $\mathbf{P} = \mathbf{Q}^T$.

The control objective is to seek an appropriate control profile that specifies the on-ramp traffic flow $r_{I_p}(k)$ that drives the traffic density of sections $\mathbf{I}_p$ at time k to converge to the desired traffic density $\rho_{I_p,desired}(k)$ for $k \in \{0, 1, \ldots, K\}$, despite the modeling uncertainties and disturbances occurring at some off-ramps.

III. Iterative Learning Control-Based Ramp Metering and Complementary Modularized Designing Based on Iterative Learning Control and ALINEA

A. State Space Representation and Assumptions

The macroscopic traffic flow model described by (1) and (2) can be written in the following form:

$$\begin{aligned}\rho_i(k+1) &= \rho_i(k) + \frac{T}{L_i}\left(v_{i-1}(k)\rho_{i-1}(k) - \rho_i(k)v_i(k) + r_i(k) - s_i(k)\right)\\ &= \left(1 - \frac{T}{L_i}v_i(k)\right)\rho_i(k) + \frac{T}{L_i}v_{i-1}(k)\rho_{i-1}(k) + \frac{T}{L_i}r_i(k) - \frac{T}{L_i}s_i(k)\\ &= a_i(k)\rho_i(k) + b_i(k)\rho_{i-1}(k) + c_i(k)r_i(k) - c_i(k)s_i(k)\end{aligned} \tag{9}$$

where $a_i(k) = 1 - (T/L_i)v_i(k)$, $b_i(k) = (T/L_i)v_{i-1}(k)$, and $c_i(k) = (T/L_i)$.

Denoting

$$\begin{aligned}\mathbf{x}(k) &= [v_1(k), v_2(k), \ldots, v_N(k)]^T\\ \mathbf{y}(k) &= [\rho_1(k), \rho_2(k), \ldots, \rho_N(k)]^T\\ \mathbf{u}(k) &= \left[r_{i_1}(k), r_{i_2}(k), \ldots, r_{i_p}(k)\right]^T\\ \mathbf{s}(k) &= [s_1(k), s_2(k), \ldots s_N(k)]^T\end{aligned}$$

$$\mathbf{A}(\mathbf{x}(k)) = \begin{bmatrix} a_1(k) & 0 & \cdots & & 0\\ b_2(k) & a_2(k) & \cdots & & 0\\ 0 & b_3(k) & a_2(k) & & \\ \vdots & & & & \\ & & & b_N(k) & a_N(k)\end{bmatrix}$$

$$\mathbf{B} = \begin{bmatrix} c_1(k) & & & \\ & c_2(k) & & \\ & & \ddots & \\ & & & c_N(k)\end{bmatrix}$$

$$\boldsymbol{\eta}(\mathbf{x}(k)) = \begin{bmatrix} b_1(k)\rho_0(k)\\ 0\\ \vdots\\ 0\end{bmatrix}$$

then the model (1)–(4) can be rewritten in state space form as

$$\mathbf{x}(k+1) = \mathbf{f}(\mathbf{x}(k), \mathbf{y}(k)) \tag{10}$$

$$\mathbf{y}(k+1) = \mathbf{A}(\mathbf{x}(k))\mathbf{y}(k) + \mathbf{BPu}(k) + \boldsymbol{\eta}(\mathbf{x}(k)) - \mathbf{Bs}(k) \tag{11}$$

where $\mathbf{f}(\cdot,\cdot)$ is a corresponding vector-valued function, and $\mathbf{B} = \mathrm{diag}(T/L_1, T/L_2, \ldots, T/L_N)$. $\mathbf{s}(k)$ is the unknown leaving traffic flow on off-ramp at time k, which will be considered as the repetitive disturbance.

Throughout this paper, $\|\cdot\|$ denotes the infinite norm, i.e., for an $s \times t$ matrix $\mathbf{M}$, in which $m_{i.j}$ symbolizes its entries

$$\|\cdot\| = \max_{1\le i\le s} \sum_{j=1}^{t} |m_{i,j}|.$$

Before showing the main results of the proposed discrete ILC system, we define the λ norm of a vector $\mathbf{u}(k)$ as

$$\|\mathbf{u}(k)\|_\lambda = \sup_{k\in[0,K]} a^{-\lambda k} \|\mathbf{u}(k)\|$$

where $\lambda > 0$, and $a > 1$.

Assumption 1: The functions $\mathbf{f}(\cdot,\cdot)$, $\mathbf{A}(\mathbf{x}(k))$, and $\boldsymbol{\eta}(\mathbf{x}(k))$ are uniformly globally Lipschitz on a bounded compact set $\boldsymbol{\Omega} = \mathbf{X} \times \mathbf{Y}$ with respect to their arguments for $k \in [0, K]$, i.e.,

$$\begin{aligned}
&\|\Re\mathbf{f}(\mathbf{x}_1(k), \mathbf{y}_1(k)) - \Re\mathbf{f}(\mathbf{x}_2(k), \mathbf{y}_2(k))\| \\
&\quad \le k_x \|\Re(\mathbf{x}_1(k) - \mathbf{x}_2(k))\| + k_y \|\Re(\mathbf{y}_1(k) - \mathbf{y}_2(k))\| \\
&\|\Re\mathbf{A}(\mathbf{x}_1(k)) - \Re\mathbf{A}(\mathbf{x}_2(k))\| \le k_A \|\Re(\mathbf{x}_1(k) - \mathbf{x}_2(k))\| \\
&\|\Re\boldsymbol{\eta}(\mathbf{x}_1(k)) - \Re\boldsymbol{\eta}(\mathbf{x}_2(k))\| \le k_\eta \|\Re(\mathbf{x}_1(k) - \mathbf{x}_2(k))\|
\end{aligned} \tag{12}$$

where k_x, k_y, k_A, and k_η are Lipschitz constants. $\mathbf{X}$ and $\mathbf{Y}$ are the ranges of speed and density of the traffic flow on the freeway, respectively.

Assumption 2: The reinitialization condition is satisfied throughout the repeated iterations, i.e.,

$$\mathbf{x}_n(0) = \mathbf{x}_d(0), \quad \mathbf{y}_d(0) = \mathbf{y}_n(0) \qquad \forall n$$

where $\mathbf{x}_d(0)$ is the initial value of the desired state, and n is the iteration number for ILC.

Assumption 3: There exists a control profile $\mathbf{u}_d(k)$ that can exactly drive the system output to track the desired trajectory $\Re\mathbf{y}_d(k)$ for systems (10) and (11) over the finite time interval $[0, K]$.

Assumption 1 requires the traffic model be globally Lipschitz continuous, which is satisfied in our case because the traffic flow model (1)–(4) is continuously differentiable in all arguments on any bounded compact set $\boldsymbol{\Omega}$. Moreover, the system states (density and mean speed) cannot be infinite in practice. In addition, the time interval is also finite. This leads to the bounded compact set $\boldsymbol{\Omega}$. Assumption 2 demands the initial state values to be consistent with the desired value. In practice, if this condition is not met, then we can always align the target trajectory with the actual trajectory at the initial stage of tracking [20]. Assumption 3 is a reasonable assumption that the task should be solvable.

B. Pure ILC Strategy

The pure ILC law for the freeway traffic local ramp is constructed as follows:

$$\mathbf{u}_{n+1}(k) = \mathbf{u}_n(k) + \boldsymbol{\beta}\Re\mathbf{e}_n(k+1) \tag{13}$$

where n indicates the iteration number, and $\boldsymbol{\beta}$ is an iterative learning gain matrix. $\mathbf{e}_n(k+1) = \mathbf{y}_d(k+1) - \mathbf{y}_n(k+1)$, and $\mathbf{y}_d(k)$ is the desired output signal (density) at time k.

Theorem 1: Under Assumptions 1–3, choosing the learning gain matrix $\boldsymbol{\beta}$ such that $\|\mathbf{I}_{p\times p} - \boldsymbol{\beta}\mathbf{Q}\mathbf{B}\mathbf{P}\| < 1$ in the ILC law (13), the mapped output of the traffic system (10) and (11) will converge to the desired output along the iteration axis, i.e.,

$$\Re\mathbf{y}_n(k) \to \Re\mathbf{y}_d(k) \text{ as } n \to \infty \qquad \text{for all } k = 1, 2, \ldots, K.$$

Proof: The proof is similar to that of Theorem 2 and, hence, is omitted. ■

Remark 1: According to the traffic model, the scope of $\boldsymbol{\beta}$ can easily be determined. Note that the $\mathbf{B}$ matrix is diagonal, and all the parameters L_{i_j} and T are known *a priori*. The learning gain matrix becomes $\boldsymbol{\beta} = \mathrm{diag}(\beta_{i_1}, \beta_{i_2}, \ldots, \beta_{i_p})$, where β_{i_j} is a scalar satisfying the following relation:

$$0 < \beta_{i_j} < \frac{2L_{i_j}}{T}.$$

Remark 2: It is interesting to note that the learning convergence is solely depending on the known parameters L_{i_j} and T. The other system parameters, such as τ, ν, κ, l, m, and ω, whose exact values may not be available, will not affect the learning convergence. Therefore, ILC is suitable for traffic control when model mismatching exists. Moreover, the exogenous disturbances $\mathbf{s}(k)$ will be eliminated entirely by the learning control and will therefore not affect the learning convergence.

C. ILC Add-On to ALINEA

In ramp metering control, feedback-based methods, such as ALINEA [3], have been developed and implemented over a long period. It would be inappropriate to completely replace the existing feedback control algorithms with ILC. Instead, we seek the combination of feedback and ILC, in which ILC is an add-on component to the existing control system. Thus, we can retain the functionality of the existing feedback loop and meanwhile enjoy the extra performance improvement from ILC. The block diagram of such a combined controller is demonstrated in Fig. 2. Note that, in addition to the inner feedback loop, ILC constitutes an outer loop along the iteration axis, as the learning correction term is generated in the nth iteration and fed to the next iteration. Mathematically, such a control strategy is expressed as follows:

$$\mathbf{u}_n(k) = \mathbf{u}_n^b(k) + \mathbf{u}_n^f(k) \tag{14}$$

$$\begin{cases} \mathbf{u}_n^b(0) = \boldsymbol{\varphi}\Re\mathbf{e}_n(0), & \text{if } k = 0 \\ \mathbf{u}_n^b(k) = \mathbf{u}_n^b(k-1) + \boldsymbol{\varphi}\Re\mathbf{e}_n(k), & \text{if } k > 0 \end{cases} \text{(ALINEA)} \tag{15}$$

$$\mathbf{u}_n^f(k) = \mathbf{u}_{n-1}(k) + \boldsymbol{\beta}\Re\mathbf{e}_{n-1}(k+1) \tag{16}$$

where $\mathbf{u}_n^f(k)$ denotes the ILC part, and $\mathbf{u}_n^b(k)$ is the ALINEA, and $\boldsymbol{\varphi}$ is the feedback gain of ALINEA.

The convergence property of the preceding control mechanism is subsequently summarized.

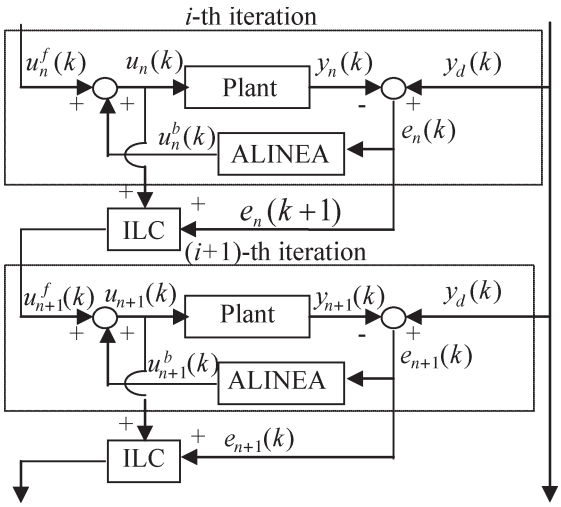

Fig. 2. Block diagram of the learning control strategy with a feedback ALINEA controller.

Theorem 2: Under Assumptions 1–3, choosing the learning gain matrix $\boldsymbol{\beta}$ such that $\|\mathbf{I}_{p\times p} - \boldsymbol{\beta}\mathbf{Q}\mathbf{B}\mathbf{P}\| < 1$ in the learning law (16), the mapped output of the traffic system (10) and (11), which is controlled by ILC (16) together with ALINEA (15), will converge to the desired output along the iteration axis, i.e.,

$$\Re\mathbf{y}_n(k) \to \Re\mathbf{y}_d(k) \text{ as } n \to \infty \qquad \text{for all } k = 1, 2, \ldots, K.$$

Proof: See Appendix A. ■

Remark 3: ILC complements ALINEA in two aspects. First, from (15), we can observe that ALINEA is a discrete-time integrator, which is effective to eliminate constant offset but less effective for time-varying disturbances. Since ILC is a point-wise integral control, it is effective in coping with time-varying disturbances that repeat daily and weekly. Second, ALINEA is a current cycle feedback that provides the control system with the desired robustness property, whereas ILC is a feedforward compensation that essentially provides a kind of prediction based on the entire operation period of previous control actions. Owing to the complementary functions, we can expect a better performance by the integrated control (14) in comparison with either ALINEA (15) or pure ILC (16).

Remark 4: Repeating the proof of Theorem 2, we can derive the proof for Theorem 1 by simply letting the ALINEA feedback part be zero.

Remark 5: From (A.21) in Appendix A, we can observe that $\|\mathbf{u}_n^b(k-1)\|_\lambda \to 0$ when the learning converges. This implies that the control system will be dominated by feedforward, and the ALINEA feedback is effectively off. This is consistent with the feature of most intelligent control systems.

Remark 6: Note that the learning controller design and the convergence condition are independent of the stabilizing controller ALINEA. On the other hand, at any iteration, what the ILC generates are exogenous signals to the ALINEA; hence, the closed-loop feedback characteristics retains. In other words, ALINEA and ILC concurrently work as two independent modules without interfering with each other. Thus, whenever necessary, we can simply switch off either of the control module and the remaining module will still perform well.

IV. Iterative Learning Control-Based Ramp Metering and Modularized Designing Based on Iterative Learning Control and ALINEA With Constraints

In practice, the ramp metering would be constrained by either the saturation flow of the ramp, which depends on the design of the ramp infrastructure, or by the actually available traffic demand of the on-ramp. On the other hand, the ramp flow should be larger than, at least, nonnegative values. Furthermore, even if Assumption 3 holds with $\mathbf{u}_d(k)$ satisfying the two preceding constraints, there is no guarantee that the actual control input at the nth iteration, that is, $\mathbf{u}_n(k)$, could satisfy the two input constraints. Therefore, it is necessary to explore the ILC-based density control to the scenario where the ramp flow $\mathbf{u}_n(k)$ is bounded by certain upper and lower limits.

Assumption 4: For the input constraints $\mathbf{u}_{\min}(k)$ and $\mathbf{u}_{\max}(k)$, the following saturator should be considered in the control law (13):

$$sat\left[\mathbf{u}_n(k)\right] = \begin{cases} \mathbf{u}_n(k), & 0 < \mathbf{u}_{\min}(k) < \mathbf{u}_n(k) < \mathbf{u}_{\max}(k) \\ \mathbf{u}_{\max}(k), & \mathbf{u}_n(k) \geq \mathbf{u}_{\max}(k) \\ \mathbf{u}_{\min}(k), & \mathbf{u}_n(k) \leq \mathbf{u}_{\min}(k). \end{cases}$$

■

In practice, the choosing of these two values of $\mathbf{u}_{\min}(k)$ and $\mathbf{u}_{\max}(k)$ depends on practical experience and the on-ramp infrastructure. Usually, $\mathbf{u}_{\min}(k)$ is set to be the minimum entering rate to make drivers know the on-ramp is not closed, and the $\mathbf{u}_{\max}(k)$ is set according to the cases how many lanes does the on-ramp has.

Before investigating learning properties under input constraints, let us first derive an important and highly correlated lemma.

Lemma 1 [9]: Under Assumptions 3 and 4, we have

$$\|\mathbf{u}_d(k) - sat\left[\mathbf{u}_n(k)\right]\| \leq \|\mathbf{u}_d(k) - \mathbf{u}_n(k)\|.$$

The system output dynamics (11) under saturation is

$$\mathbf{y}(k+1) = \mathbf{A}\left(\mathbf{x}(k)\right)\mathbf{y}(k) + \mathbf{B}\mathbf{P}sat\left[\mathbf{u}(k)\right] + \boldsymbol{\eta}\left(\mathbf{x}(k)\right) - \mathbf{B}\mathbf{s}(k). \tag{17}$$

The ILC law (13) under input constraints becomes

$$\mathbf{u}_{n+1}(k) = sat\left[\mathbf{u}_n(k)\right] + \boldsymbol{\beta}\Re\mathbf{e}_n(k+1). \tag{18}$$

The traffic control property with the pure ILC law (18) is summarized in the following theorem.

Theorem 3: Under Assumptions 1–4, choosing the learning gain matrix $\boldsymbol{\beta}$ of (18) such that $\|\mathbf{I}_{p\times p} - \boldsymbol{\beta}\mathbf{Q}\mathbf{B}\mathbf{P}\| < 1$, the output of the traffic system (10) and (17) will iteratively converge to the desired output, i.e.,

$$\Re\mathbf{y}_n(k) \to \Re\mathbf{y}_d(k),\ n \to \infty \qquad \text{for all } k = 1, 2, \ldots, K.$$

Proof: The proof is similar to that of Theorem 4 and hence omitted.

Now, let us discuss the traffic performance where ILC is added to ALINEA subject to input constraints. The original updating law (14)–(16) is modified with the saturator

$$\mathbf{u}_n(k) = \mathbf{u}_n^f(k) + \mathbf{u}_n^b(k) \tag{19}$$

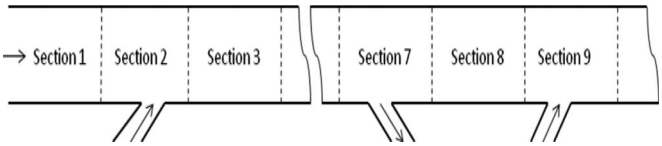

Fig. 3. Schematic diagram of the simulated freeway.

$$\begin{cases} \mathbf{u}_n^b(0) = \boldsymbol{\varphi}\Re\mathbf{e}_n(0), & \text{if } k = 0 \\ \mathbf{u}_n^b(k) = \mathbf{u}_n^b(k-1) + \boldsymbol{\varphi}\Re\mathbf{e}_n(k), & \text{if } k > 0 \end{cases} \tag{20}$$

$$\mathbf{u}_n^f(k) = sat\left(\mathbf{u}_{n-1}(k)\right) + \boldsymbol{\beta}\Re\mathbf{e}_{n-1}(k+1). \tag{21}$$

The traffic control property with this modified control law is summarized in the following theorem. ■

Theorem 4: Under Assumptions 1–4, using control laws (19)–(21) with the learning gain matrix $\boldsymbol{\beta}$ such that $\|\mathbf{I}_{p\times p} - \boldsymbol{\beta}\mathbf{QBP}\| < 1$, the output of the traffic system (10) and (17) will iteratively converge to the desired output, i.e.,

$$\Re\mathbf{y}_n(k) \to \Re\mathbf{y}_d(k)\ k \in [0, K],\ n \to \infty.$$

Proof: See Appendix B. ■

Remark 7: It is interesting to note that, despite the presence of input constraints, ILC can still warrant an asymptotic convergent tracking performance. For some other detailed discussion, see [9] and [11]. On the other hand, the input constraints will inevitably affect the transient behavior of learning control, such as the learning convergence rate.

V. Simulation Investigations

A. Freeway Setup

The simulation settings are as follows. Consider a long segment of a single lane freeway that is divided into 12 sections, as shown in Fig. 3. The length of each section is 500 m. The initial traffic volume entering section 1 is 1500 vehicles/h. There are two on-ramps and one off-ramp in the segment, and they are located in sections 2 and 9 and in section 7, respectively.

The desired density was $y_d = 30$ vehicles/lane/km. The freeway system is in the presence of a large exogenous disturbance (modeled by an exiting flow in an off-ramp during a period and other random disturbance). It is worthwhile pointing out that model-based optimal control or pure error feedback is not able to completely reject the influence for such an unknown exogenous disturbance. Further, even if the disturbance is known, it is still difficult to find an appropriate control profile due to the highly nonlinear and uncertain factors in the traffic model.

The initial density and mean speed of each section are set as shown in Table I, and the parameters used in the model are also listed in this table. From the table, we can see that the initial values of density and speed are not in their equilibrium position according to the initial flow volume, that is, the initial ILC convergence condition $\Re\delta x(0) = 0$ is not strictly satisfied. This setting thus shows the robustness of the proposed control schemes to the initial set values.

TABLE I
Initial Values and Parameters With the Traffic Model

Section	$\rho_i(0)$	$v_i(0)$	Parameters	
1	30	50	v_{free} (km/h)	80
2	30	50	ρ_{jam} (veh/lane/km)	80
3	30	50	l	1.8
4	30	50	m	1.7
5	30	50	κ (veh/km)	13
6	30	50	τ (h)	0.01
7	30	50	T (h)	0.00417
8	30	50	ν (km^2/h)	35
9	30	50	$q_0(k)$ (veh/h)	1500
10	30	50	$r_i(0)$ (veh/h)	0
11	30	50	ω	0.95
12	30	50		

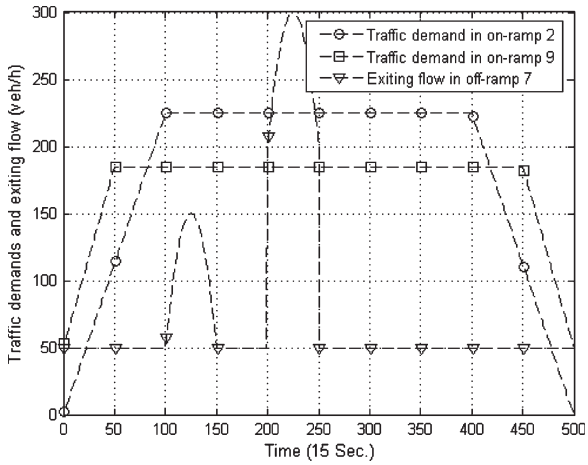

Fig. 4. Known traffic demands and unknown exiting flow in off-ramp that violates Assumption 3.

B. Traffic Demand Patterns

The setting of the traffic demand patterns (on-ramp) and outflow pattern (off-ramp) should be able to simulate the traffic practical situation during routine or rush hour. The traffic demand pattern setup in this paper is to show that Assumption 3 is necessary and sufficient for the perfect tracking of the proposed ILC-based control strategies.

When Assumption 3 is satisfied, the theoretical analysis has shown that convergence has been achieved. Due to page limitations, here, we just simulate the situation that the traffic demands are inadequate.

Inadequate demand means that Assumption 3 is not satisfied. In other words, the on-ramp queuing demands impose constraints on the control inputs. Due to the constraints from insufficient traffic demands in on-ramps 2 and 9, the on-ramp flows resulting from the controller are truncated if the calculated on-ramp flow exceeds the on-ramp queuing traffic demand. In such circumstances, $\mathbf{u}_d(k)$ is not reachable. Since Assumption 3 is violated, we cannot expect perfect flow tracking. The inadequate demands are shown in Fig. 4.

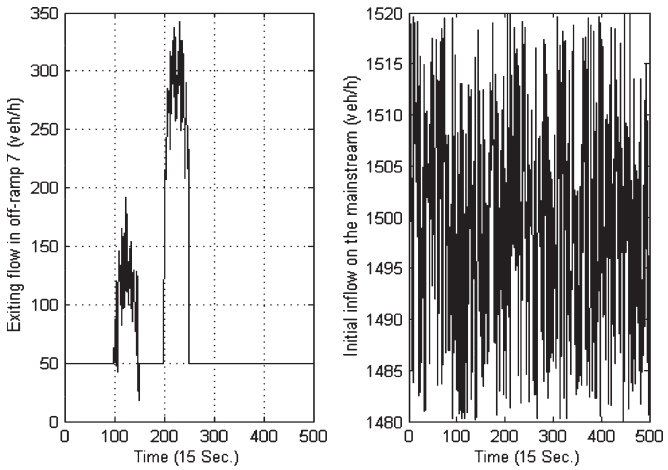

Fig. 5. Exiting flow and initial inflow with random disturbance.

Note that the queuing demands actually impose constraints on the control inputs of ramp metering, i.e., the on-ramp volumes cannot exceed the current demands plus the existing waiting queues at on-ramps $i \in I_{\rm on}$ at time k; thus

$$r_i(k) \le d_i(k) + \frac{l_i(k)}{T}, \qquad i \in I_{\rm on}$$

where $l_i(k)$ denotes the length (in vehicles) of a possibly existing waiting queue at time k at the ith on-ramp, $d_i(k)$ is the demand flow at time k at the ith on-ramp (in vehicles per hour), and $I_{\rm on} = \{2, 9\}$ denotes the set of indices of the sections where an on-ramp exists. On the other hand, the waiting queue is the accumulation of the difference between the demands and the actual on-ramp, i.e.,

$$l_i(k+1) = l_i(k) + T\left[d_i(k) - r_i(k)\right], \qquad i \in I_{\rm on}.$$

C. Scenarios and Cases

Two scenarios are simulated under inadequate traffic demands in the on-ramps.

Scenario A: The traffic system is strict repeatable. Traffic control with strict day-to-day repeatability is the most ideal scenario. The purpose of this scenario is to show the effectiveness and correctness for the proposed ILC methods under the ideal settings.

Scenario B: The traffic system is not strict repeatable, which is simulated by adding random disturbances in states, initial mainstream inflows, and exiting flows. The nonrepeatable disturbances are random state disturbances uniformly distributed on the interval $(-0.5, 0.5)$ and are added to the right side of the state equations (10), that is, the dynamic speed equations of the traffic flow. A random disturbance uniformly distributed on the interval $(-50, 50)$ is added to the unknown exiting flow in off-ramp 7 from time instants 100–150 and 200–250, respectively. A random disturbance uniformly distributed on the interval $(-40, 40)$ is added to the initial traffic inflow on the mainstream for all the time instants, which are shown in Fig. 5. This scenario is to show the robustness of the ILC-based control schemes with respect to various nonrepeatable factors.

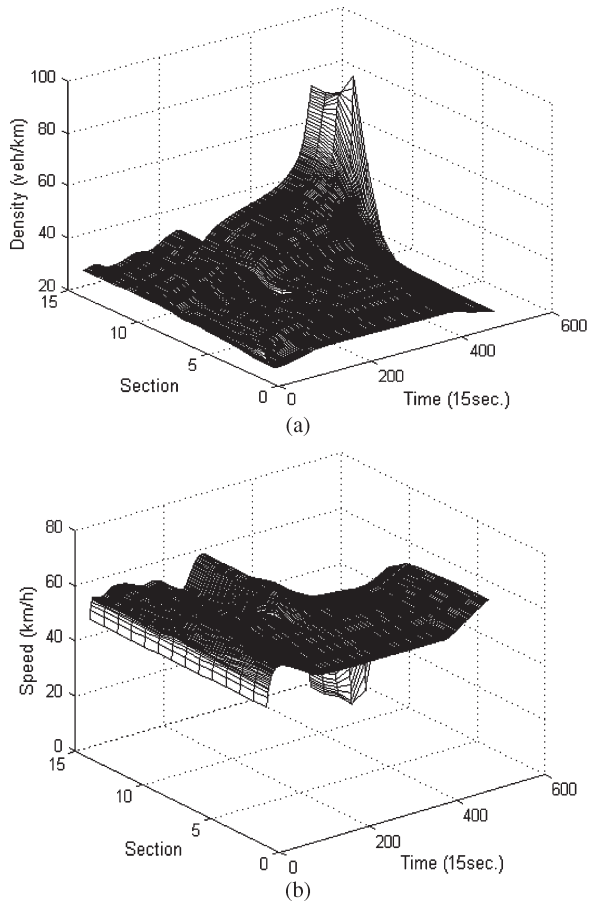

Fig. 6. Simulation results of Case A-I. (a) Density profile with no control. (b) Speed profile with no control.

D. Investigations

Scenario A—Traffic Control With Strict Day-to-Day Repeatability Under Inadequate Demands: In practical traffic flow, the actual available traffic demand may be lower than the desired entering flow at a specific on-ramp. That is, there does not exist a control profile $u_d(k) = [r_2(k), r_9(k)]^T$ that can exactly drive the system output to the desired trajectory $\Re y_d(k) = [30, 30]^T$ for the systems (10) and (11) over the finite time interval [0, K]. This implies that Assumption 3 is violated, and we cannot expect perfect flow control. Despite this limitation, it would be meaningful to investigate whether the new approach still works. In this scenario, we simulate the freeway traffic with on-ramp traffic demands and off-ramp exiting flow, as shown in Fig. 4.

In this scenario, the investigations focus on the following two issues.

1) The ILC-based schemes are still effective when the traffic system is strict repeatable under inadequate traffic demands.
2) Performance comparison of ALINEA, pure ILC, and ILC+ALINEA in this scenario.

Four cases are simulated. Case A-I is the no control case, Case A-II is the ALINEA alone case, Case A-III is the pure

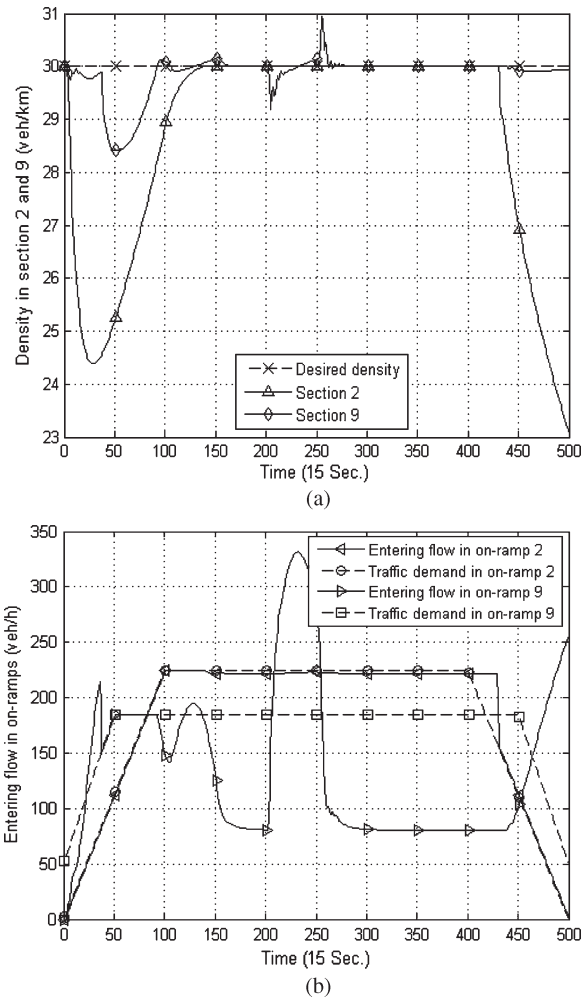

Fig. 7. Simulation results of Case A-II. (a) Density tracking performance in on-ramps 2 and 9. (b) Entering flows in on-ramps 2 and 9.

ILC case, and Case A-IV is the ILC add-on to existing ALINEA case.

Case A-I—No Control: The traffic flow on the mainstream evolved by the traffic demands in on-ramps 2 and 9, as well as the exiting flow in off-ramp 7, is shown in Fig. 6. Without control, the density reaches the maximum jam density, and traffic jam occurs, resulting in an almost zero speed.

Case A-II—ALINEA Control: The ALINEA gains for sections 2 and 9 are chosen to be $\boldsymbol{\varphi} = \mathrm{diag}(40, 40)$, as suggested in [1] and [3], which gives the best performance.

To overcome the integral saturation action of ALINEA, an antisaturation measurement, as suggested in [1], is incorporated. As such, the on-ramp flows calculated according to ALINEA control law will be truncated if they exceed the on-ramp queuing traffic demands in on-ramps 2 and 9. By truncation, the on-ramp flow values will be kept the same as that of the preceding instant, i.e., $u_n^b(k-1)$. Fig. 7 shows the simulation results. From Fig. 7(a), we can see that the traffic has been controlled at the desired level by ALINEA control, and a pretty good tracking performance is obtained. The lower departures from time instant 0 to about 100 and from 440 to end both for sections 2 and 9 in Fig. 7(a) are caused by the insufficient traffic demands, which can be seen in corresponding parts in Fig. 7(b). However, the lower deviations at about 200 and 250 from the desired density in sections 2 and 9 are caused by the nature of the integral action of ALINEA (lack of damping) and the time delay of the process.

Case A-III—Pure ILC: The ILC gains are set to be $\boldsymbol{\beta} = \mathrm{diag}(30, 30)$. The theoretically feasible range for ILC gain is (0, 239.808) according to the learning convergence condition. The learning process is iterated for 20 cycles. The simulation results are shown in Fig. 8. Due to the constraints of insufficient traffic demands in on-ramps 2 and 9, the on-ramp flows resulting from ILC are truncated if the calculated on-ramp flow exceeds the on-ramp queuing traffic demands. Comparing Fig. 8(a) with Fig. 7(a), the improved control performance can be seen. Fig. 8(b) shows both the traffic demands and the actual entering flows in on-ramps 2 and 9, respectively. Fig. 8(c) shows the learning errors in sections 2 and 9. The deviations between the desired density and the actual density at about time instant 50 for section 9 and at the end point for section 2 (500th time instant) in Fig. 8(a) dominate the learning errors for both sections 2 and 9. Here, the learning error is defined as the maximum absolute error between the real density and the desired density over the whole period of 500 sampling instants concerned. These maximum deviations are caused by the lack of traffic demands in on-ramps 2 and 9.

Case A-IV—ILC Add-On to Existing ALINEA: Considering the insufficient on-ramp traffic demands in on-ramps 2 and 9 and the integral nature of both ALINEA and ILC, the control saturation problem may be worsened in this case. Taking the conclusion of Remark 5 into consideration, an immediate remedy is to shape the ALINEA gain to a lower level as the iteration increases, and let ILC action gradually take a larger share. A simple way is to modify the ALINEA gain to be $\boldsymbol{\varphi} = \mathrm{diag}(40e^{-(n-1)}, 40e^{-(n-1)})$, where n is the number of iterations. The ILC learning gains are $\boldsymbol{\beta} = \mathrm{diag}(30, 30)$ for sections 2 and 9. The simulation results after 20 iterations are shown in Fig. 9. We can see a better performance comparing Fig. 9(c) with Fig. 8(c).

Furthermore, by comparing the learning performance of sections 2 and 9 [Figs. 8(c) and 9(c)], it is clear that the combined ALINEA plus ILC gives better results and faster convergence speeds, since Case A-IV shows much lower tracking errors in the first iteration by feedback, whereas Case A-III has larger errors in the first iteration due to the open-loop.

From the simulations of scenario A, we can conclude that, if the traffic system is strict repeatable, and Assumption 3 is violated, that is, $\mathbf{u}_d(k)$ is unreachable, perfect tracking cannot be achieved in any case. However, the deviations between the desired density and the actual density are just caused by the lack of demands. Traffic jams can still be avoided by these control methods. The ILC+ALINEA method is the best in this situation with the best density tracking ability and the least tracking errors to that of ALINEA alone and the pure ILC case.

Scenario B—ILC-Based Traffic Control Having Nonrepeatable Disturbance and Inadequate Demands: In this scenario, we simulate the same freeway traffic as scenario A, except for the nonrepeatable stochastic disturbances.

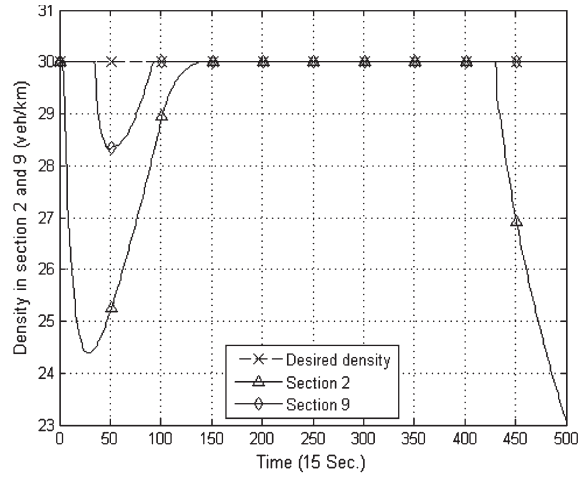

(a)

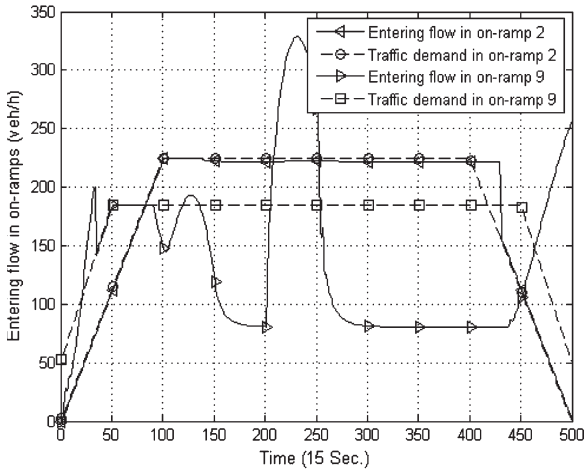

(b)

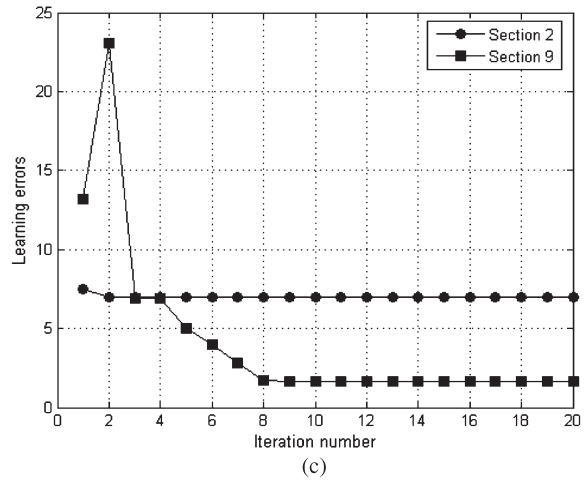

(c)

Fig. 8. Simulation results of Case A-III. (a) Density tracking performance in on-ramps 2 and 9 at the 20th iteration. (b) Entering flows in on-ramps 2 and 9 at the 20th iteration. (c) Iterative errors in sections 2 and 9.

This scenario investigation mainly focuses on two issues.

1) The effectiveness of ILC-based schemes when the traffic system has nonrepeatable stochastic disturbance in state, initial mainstream inflow and exiting flow under inadequate demands.
2) The performance comparison between the pure ILC and ILC+ALINEA.

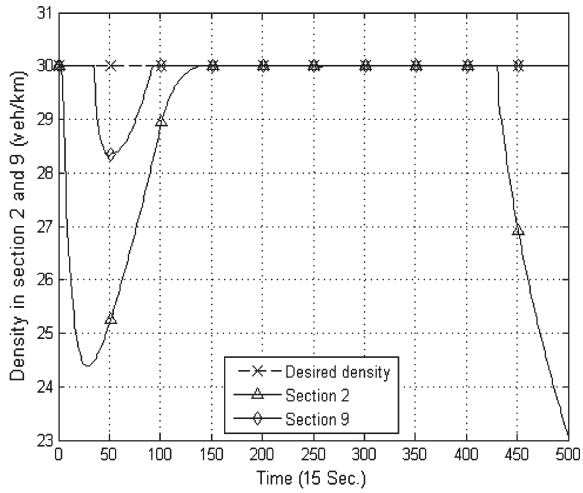

(a)

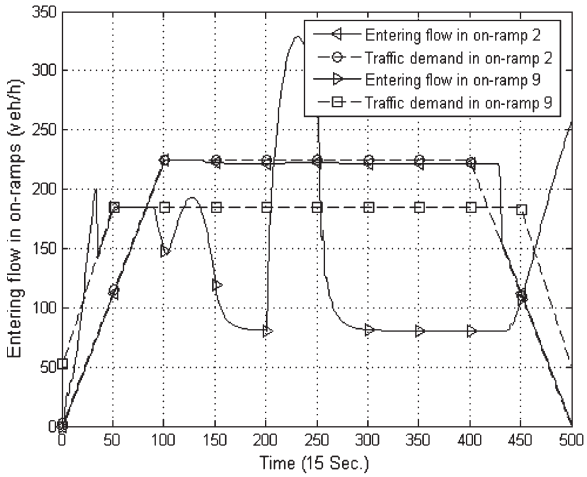

(b)

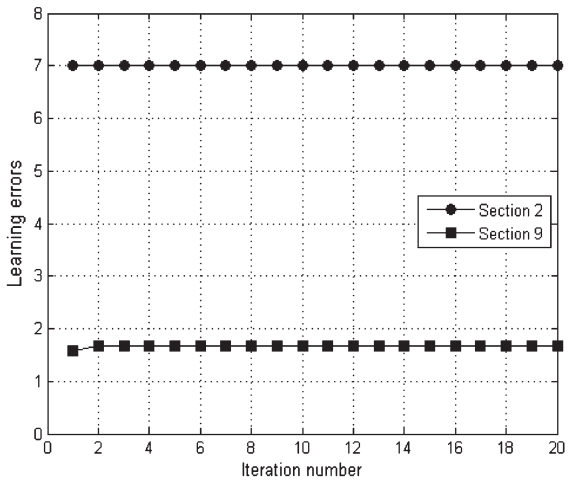

(c)

Fig. 9. Simulation results of Case A-IV. (a) Density tracking performance in on-ramps 2 and 9 at the 20th iteration. (b) Entering flows in on-ramps 2 and 9 at the 20th iteration. (c) Iterative errors in sections 2 and 9.

Two cases are simulated in this part. Case B-I is the pure ILC case, and Case B-II is the ILC add-on to existing ALINEA case.

Case B-I—Pure ILC With Random Disturbances in State, Initial Mainstream Inflow, and Exiting Flow: The ILC gains are set to be $\boldsymbol{\beta} = \mathrm{diag}(30, 30)$. The learning process is

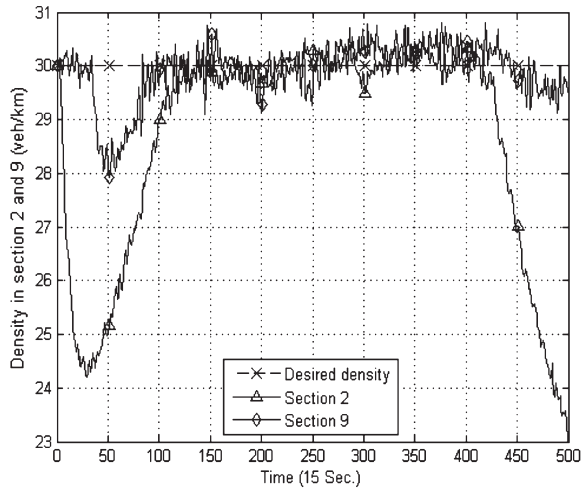

(a)

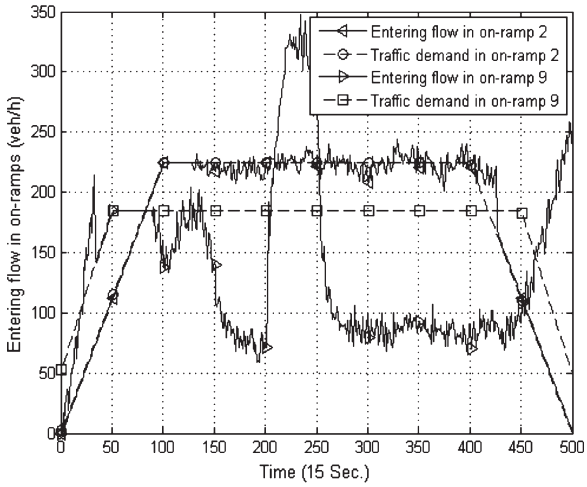

(b)

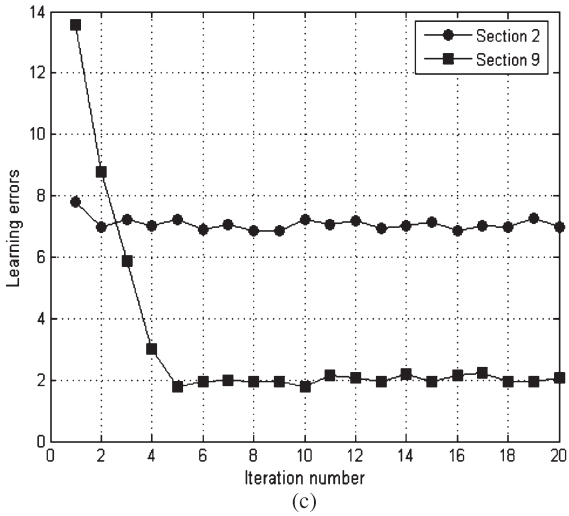

(c)

Fig. 10. Simulation results of Case B-I. (a) Density tracking performance in on-ramps 2 and 9 at the 20th iteration. (b) Entering flows in on-ramps 2 and 9 at the 20th iteration. (c) Iterative errors in sections 2 and 9.

iterated for 20 cycles, and the simulation results are shown in Fig. 10. The time domain control response can be observed from Fig. 10(a), and the effective tracking can still be seen although the traffic is with nonrepeatable factors.

Case B-II—ILC Add-On to Existing ALINEA With Random Disturbances in State, Initial Mainstream Inflow, and Exiting Flow: The learning law is integrated with the existing ALINEA controller, whose gain is $\boldsymbol{\varphi} = \mathrm{diag}(40e^{-(n-1)}, 40e^{-(n-1)})$, where n is the number of iterations. The ILC learning gains are $\boldsymbol{\beta} = \mathrm{diag}(30, 30)$ for sections 2 and 9. The simulation results after 20 iterations are shown in Fig. 11. Despite the large random factors, the tracking error is kept at a low level. Comparing with Fig. 10(c) of Case B-I, the error is lower in this case, as shown in Fig. 11(c), which benefits from the help of feedback ALINEA in the first few iterations.

From the simulation results of Scenario B, we can see that the ILC-based control strategies have a very strong robustness to the nonrepeatable disturbed traffic patterns. In other words, they can still work well without the strict repeatability condition.

VI. Conclusion

In this paper, we have applied ILC to address local ramp metering in a macroscopic-level freeway environment by formulating the ramp metering problem as output tracking, disturbance rejection, and input constrained problems. For the freeway traffic system with a strict repeatable pattern, the ILC-based approach has been successfully applied to solve the ramp control problems. The learning mechanism is further combined with ALINEA in a complementary manner to guarantee the desired perfect tracking performance. Then, the ILC-based ramp metering and the complementary modularized designing method based on ILC and ALINEA under input constraint are also analyzed. Case studies with intensive simulations on a macroscopic-level freeway model confirm the validity of the proposed approaches. For the freeway traffic system without a repeatable pattern represented by iteration-varying or time-varying parameters and desired density trajectory, the corresponding modified ILC-based control schemes will be published in other work.

Appendix A
Proof of Theorem 2

The ILC is

$$\mathbf{u}_{n+1}^{f}(k) = \mathbf{u}_n(k) + \boldsymbol{\beta}\Re\mathbf{e}_n(k+1) \tag{A.1}$$

$$\begin{cases} \mathbf{u}_n^b(0) = \boldsymbol{\varphi}\Re\mathbf{e}_n(0), & \text{if } k = 0 \\ \mathbf{u}_n^b(k) = \mathbf{u}_n^b(k-1) + \boldsymbol{\varphi}\Re\mathbf{e}_n(k), & \text{if } k > 0 \end{cases} \tag{A.2}$$

$$\mathbf{u}_n(k) = \mathbf{u}_n^b(k) + \mathbf{u}_n^f(k). \tag{A.3}$$

Defining

$$\begin{aligned} \delta\mathbf{u}_n^f(k) &= \mathbf{u}_d(k) - \mathbf{u}_n^f(k) \\ \delta\mathbf{x}_n(k) &= \mathbf{x}_d(k) - \mathbf{x}_n(k) \\ \delta\mathbf{u}_n(k) &= \mathbf{u}_d(k) - \mathbf{u}_n(k) \\ \delta\mathbf{A}\left(\mathbf{x}_n(k)\right) &= \mathbf{A}\left(\mathbf{x}_d(k)\right) - \mathbf{A}\left(\mathbf{x}_n(k)\right) \\ \delta\boldsymbol{\eta}\left(\mathbf{x}_n(k)\right) &= \boldsymbol{\eta}\left(\mathbf{x}_d(k)\right) - \boldsymbol{\eta}\left(\mathbf{x}_n(k)\right) \end{aligned}$$

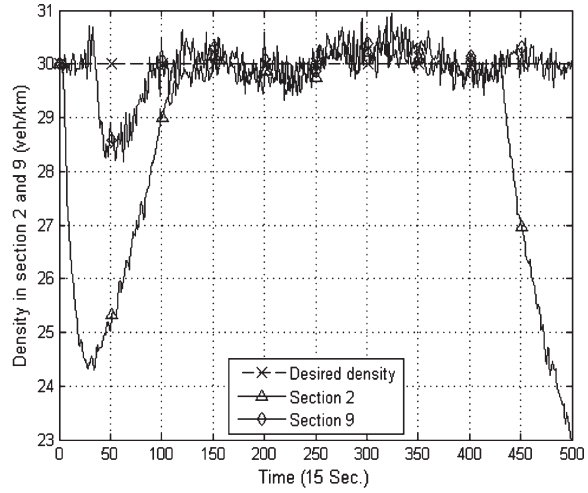

(a)

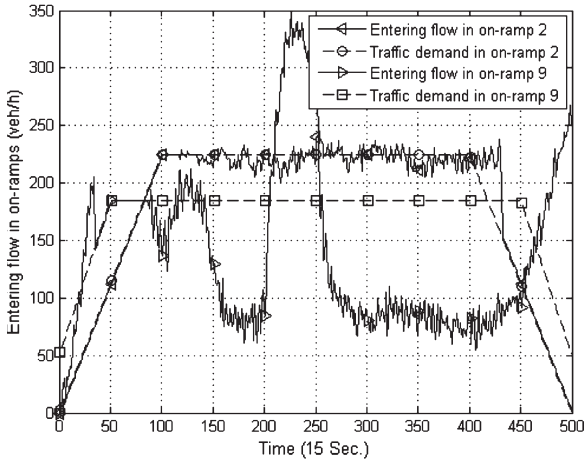

(b)

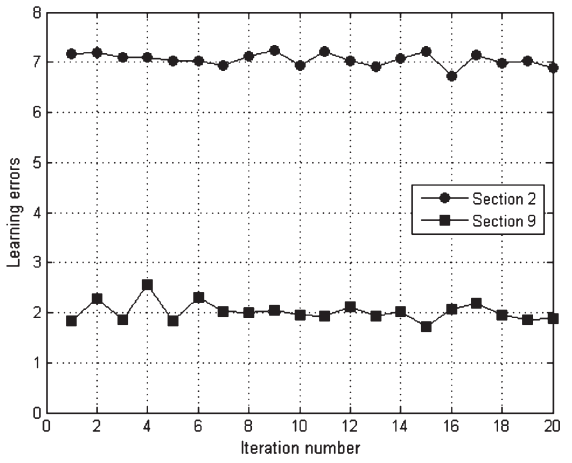

(c)

Fig. 11. Simulation results of Case B-II. (a) Density tracking performance in on-ramp 2 and 9 at the 20th iteration. (b) Entering flow in on-ramp 2 and 9 at the 20th iteration. (c) Learning errors in section 2 and 9.

then

$$\begin{aligned}\delta\mathbf{u}_{n+1}^{f}(k) &= \mathbf{u}_d(k) - \mathbf{u}_{n+1}^{f}(k)\\ &= \mathbf{u}_d(k) - \mathbf{u}_n(k) - \boldsymbol{\beta}\Re\mathbf{e}_n(k+1)\\ &= \delta\mathbf{u}_n(k) - \boldsymbol{\beta}\Re\mathbf{e}_n(k+1). \end{aligned} \tag{A.4}$$

Using (11) and Assumption 3, we have

$$\begin{aligned}\Re\mathbf{e}_n(k+1) &= \Re\{\mathbf{A}(\mathbf{x}_d(k))\mathbf{y}_d(k) + \mathbf{BP}\mathbf{u}_d(k)\\ &\quad + \boldsymbol{\eta}(\mathbf{x}_d(k)) - \mathbf{Bs}(k) - \mathbf{A}(\mathbf{x}_n(k))\mathbf{y}_n(k)\\ &\quad - \mathbf{BP}\mathbf{u}_n(k) - \boldsymbol{\eta}(\mathbf{x}_n(k)) + \mathbf{Bs}(k)\}\\ &= \Re\{\mathbf{A}(\mathbf{x}_d(k))\mathbf{y}_d(k) - \mathbf{A}(\mathbf{x}_n(k))\mathbf{y}_d(k)\\ &\quad + \mathbf{A}(\mathbf{x}_n(k))\mathbf{y}_d(k) - \mathbf{A}(\mathbf{x}_n(k))\mathbf{y}_n(k)\\ &\quad + \mathbf{BP}\mathbf{u}_d(k) + \boldsymbol{\eta}(\mathbf{x}_d(k))\\ &\quad - \mathbf{BP}\mathbf{u}_n(k) - \boldsymbol{\eta}(\mathbf{x}_n(k))\}\\ &= \Re\{\delta\mathbf{A}(\mathbf{x}_n(k))\mathbf{y}_d(k) + \mathbf{A}(\mathbf{x}_n(k))\mathbf{e}_n(k)\\ &\quad + \mathbf{BP}\delta\mathbf{u}_n(k) + \delta\boldsymbol{\eta}(\mathbf{x}_n(k))\}\\ &= \Re[\delta\mathbf{A}(\mathbf{x}_n(k))\mathbf{y}_d(k)] + \Re[\mathbf{A}(\mathbf{x}_n(k))\mathbf{e}_n(k)]\\ &\quad + \mathbf{QBP}\delta\mathbf{u}_n(k) + \Re[\delta\boldsymbol{\eta}(\mathbf{x}_n(k))]. \end{aligned} \tag{A.5}$$

Substituting (A.5) into (A.4) gives

$$\begin{aligned}&\delta\mathbf{u}_{n+1}^{f}(k)\\ &= \delta\mathbf{u}_n(k) - \boldsymbol{\beta}\Re\mathbf{e}_n(k+1)\\ &= \delta\mathbf{u}_n(k) - \boldsymbol{\beta}\{\Re[\delta\mathbf{A}(\mathbf{x}_n(k))\mathbf{y}_d(k)] + \Re[\mathbf{A}(\mathbf{x}_n(k))\mathbf{e}_n(k)]\\ &\quad + \mathbf{QBP}\delta\mathbf{u}_n(k) + \Re[\delta\boldsymbol{\eta}(\mathbf{x}_n(k))]\}\\ &= (\mathbf{I} - \boldsymbol{\beta}\mathbf{QBP})\delta\mathbf{u}_n(k) - \boldsymbol{\beta}\Re[\delta\mathbf{A}(\mathbf{x}_n(k))\mathbf{y}_d(k)]\\ &\quad - \boldsymbol{\beta}\Re[\mathbf{A}(\mathbf{x}_n(k))\mathbf{e}_n(k)] - \boldsymbol{\beta}\Re[\delta\boldsymbol{\eta}(\mathbf{x}_n(k))]. \end{aligned} \tag{A.6}$$

Since

$$\begin{aligned}\delta\mathbf{u}_n(k) &= \mathbf{u}_d(k) - \mathbf{u}_n(k)\\ &= \mathbf{u}_d(k) - \mathbf{u}_n^{f}(k) - \mathbf{u}_n^{b}(k)\\ &= \delta\mathbf{u}_n^{f}(k) - \mathbf{u}_n^{b}(k) \end{aligned} \tag{A.7}$$

$$\left\|\mathbf{u}_n^{b}(k)\right\| \le \left\|\mathbf{u}_n^{b}(k-1)\right\| + \|\boldsymbol{\varphi}\|\,\|\Re\mathbf{e}_n(k)\| \tag{A.8}$$

then using (A.7) and (A.8) and taking the norm operation for (A.6) yield

$$\begin{aligned}&\left\|\delta\mathbf{u}_{n+1}^{f}(k)\right\|\\ &\le \|\mathbf{I} - \boldsymbol{\beta}\mathbf{QBP}\| \cdot \|\delta\mathbf{u}_n(k)\| + \|\boldsymbol{\beta}\|k_A b_{y_d}\,\|\Re(\delta\mathbf{x}_n(k))\|\\ &\quad + \|\boldsymbol{\beta}\|b_A\,\|\Re\mathbf{e}_n(k)\| + \|\boldsymbol{\beta}\|k_\eta\,\|\Re(\delta\mathbf{x}_n(k))\|\\ &= \|\mathbf{I} - \boldsymbol{\beta}\mathbf{QBP}\| \cdot \|\delta\mathbf{u}_n(k)\|\\ &\quad + (\|\boldsymbol{\beta}\|k_A b_{y_d} + \|\boldsymbol{\beta}\|k_\eta)\,\|\Re(\delta\mathbf{x}_n(k))\| + \|\boldsymbol{\beta}\|b_A\,\|\Re\mathbf{e}_n(k)\|\\ &\le \|\mathbf{I} - \boldsymbol{\beta}\mathbf{QBP}\| \cdot \left\|\delta\mathbf{u}_n^{f}(k)\right\| + \|\mathbf{I} - \boldsymbol{\beta}\mathbf{QBP}\| \cdot \left\|\mathbf{u}_n^{b}(k-1)\right\|\\ &\quad + (\|\boldsymbol{\beta}\|k_A b_{y_d} + \|\boldsymbol{\beta}\|k_\eta)\,\|\Re(\delta\mathbf{x}_n(k))\|\\ &\quad + (\|\boldsymbol{\beta}\|b_A + \|\boldsymbol{\varphi}\|\,\|\mathbf{I} - \boldsymbol{\beta}\mathbf{QBP}\|\cdot)\,\|\Re\mathbf{e}_n(k)\|\\ &= \|\mathbf{I} - \boldsymbol{\beta}\mathbf{QBP}\| \cdot \left\|\delta\mathbf{u}_n^{f}(k)\right\|\\ &\quad + \varepsilon_1\left(\left\|\mathbf{u}_n^{b}(k-1)\right\| + \|\Re(\delta\mathbf{x}_n(k))\| + \|\Re\mathbf{e}_n(k)\|\right) \end{aligned} \tag{A.9}$$

where b_A and b_{y_d} are two bounded constants, and

$$\varepsilon_1 = \max_{k\in[0,K]} \{(\|\boldsymbol{\beta}\| k_A b_{y_d} + \|\boldsymbol{\beta}\| k_\eta), \|\mathbf{I} - \boldsymbol{\beta}\mathbf{Q}\mathbf{B}\mathbf{P}\| (\|\boldsymbol{\beta}\| b_A + \|\boldsymbol{\varphi}\| \|\mathbf{I} - \boldsymbol{\beta}\mathbf{Q}\mathbf{B}\mathbf{P}\|)\}.$$

From (10), we have

$$\|\Re(\delta\mathbf{x}_n(k))\| \le k_x \|\Re(\delta\mathbf{x}_n(k-1))\| + k_y \|\Re\mathbf{e}_n(k-1)\|. \tag{A.10}$$

Equation (A.2) gives

$$\left\|\mathbf{u}_n^b(k-1)\right\| \le \left\|\mathbf{u}_n^b(k-2)\right\| + \|\boldsymbol{\varphi}\| \|\Re\mathbf{e}_n(k-1)\| \tag{A.11}$$

and equations (A.5), (A.7), and (A.11) yield

$$\begin{aligned}\|\Re\mathbf{e}_n(k)\| &\le (k_A b_{y_d} + k_\eta) \|\Re(\delta\mathbf{x}_n(k-1))\| \\ &\quad + b_A \|\Re\mathbf{e}_n(k-1)\| + \|\mathbf{Q}\mathbf{B}\mathbf{P}\| \|\delta\mathbf{u}_n(k-1)\| \\ &\le (k_A b_{y_d} + k_\eta) \|\Re(\delta\mathbf{x}_n(k-1))\| + b_A \|\Re\mathbf{e}_n(k-1)\| \\ &\quad + \|\mathbf{Q}\mathbf{B}\mathbf{P}\| \left(\left\|\delta\mathbf{u}_n^f(k-1)\right\| + \left\|\mathbf{u}_n^b(k-1)\right\|\right) \\ &\le (k_A b_{y_d} + k_\eta) \|\Re(\delta\mathbf{x}_n(k-1))\| \\ &\quad + (b_A + \|\boldsymbol{\varphi}\| \|\mathbf{Q}\mathbf{B}\mathbf{P}\|) \|\Re\mathbf{e}_n(k-1)\| \\ &\quad + \|\mathbf{Q}\mathbf{B}\mathbf{P}\| \left\|\mathbf{u}_n^b(k-2)\right\| + \|\mathbf{Q}\mathbf{B}\mathbf{P}\| \left\|\delta\mathbf{u}_n^f(k-1)\right\|.\end{aligned} \tag{A.12}$$

Summing up (A.10), (A.11), and (A.12), we have

$$\begin{aligned}&\left(\left\|\mathbf{u}_n^b(k-1)\right\| + \|\Re(\delta\mathbf{x}_n(k))\| + \|\Re\mathbf{e}_n(k)\|\right) \\ &\le \varepsilon_2 \left(\left\|\mathbf{u}_n^b(k-2)\right\| + \|\Re(\delta\mathbf{x}_n(k-1))\| + \|\Re\mathbf{e}_n(k-1)\|\right) \\ &\quad + \|\mathbf{Q}\mathbf{B}\mathbf{P}\| \left\|\delta\mathbf{u}_n^f(k-1)\right\| \\ &\qquad\qquad \vdots \\ &\le \varepsilon_2^{k-1} \left(\left\|\mathbf{u}_n^b(0)\right\| + \|\Re(\delta\mathbf{x}_n(1))\| + \|\Re\mathbf{e}_n(1)\|\right) \\ &\quad + \sum_{j=1}^{k-1} \varepsilon_2^{k-j-1} \|\mathbf{Q}\mathbf{B}\mathbf{P}\| \left\|\delta\mathbf{u}_n^f(j)\right\| \\ &\le \varepsilon_2^{k} \left(\|\boldsymbol{\varphi}\| \|\Re\mathbf{e}_n(0)\| + \|\Re(\delta\mathbf{x}_n(0))\| + \|\Re\mathbf{e}_n(0)\|\right) \\ &\quad + \sum_{j=0}^{k-1} \varepsilon_2^{k-j-1} \|\mathbf{Q}\mathbf{B}\mathbf{P}\| \left\|\delta\mathbf{u}_n^f(j)\right\|\end{aligned} \tag{A.13}$$

where

$$\varepsilon_2 = \max_{k\in[0,K]} \{(k_x + k_A b_{y_d} + k_\eta), (k_y + b_A + \|\boldsymbol{\varphi}\| + \|\boldsymbol{\varphi}\| \|\mathbf{Q}\mathbf{B}\mathbf{P}\|), (\mathbf{1} + \|\mathbf{Q}\mathbf{B}\mathbf{P}\|)\}.$$

Obviously, $\varepsilon_2 > 1$.

From Assumption 2, (A.13) gives

$$\begin{aligned}&\left(\left\|\mathbf{u}_n^b(k-1)\right\| + \|\Re(\delta\mathbf{x}_n(k))\| + \|\Re\mathbf{e}_n(k)\|\right) \\ &\le \sum_{j=0}^{k-1} \varepsilon_2^{k-j-1} \|\mathbf{Q}\mathbf{B}\mathbf{P}\| \left\|\delta\mathbf{u}_n^f(j)\right\|).\end{aligned} \tag{A.14}$$

By substituting (A.14) into (A.9), we can obtain

$$\begin{aligned}\left\|\delta\mathbf{u}_{n+1}^f(k)\right\| &\le \|\mathbf{I} - \boldsymbol{\beta}\mathbf{Q}\mathbf{B}\mathbf{P}\| \left\|\delta\mathbf{u}_n^f(k)\right\| \\ &\quad + \varepsilon_1 \sum_{j=0}^{k-1} \varepsilon_2^{k-j-1} \|\mathbf{Q}\mathbf{B}\mathbf{P}\| \left\|\delta\mathbf{u}_n^f(j)\right\|.\end{aligned} \tag{A.15}$$

Multiplying $\varepsilon_2^{-\lambda k}$ on both sides of (A.15) over the interval [0, K] and taking the supreme norm result in the following relationship:

$$\begin{aligned}\sup_{k\in[0,K]} \varepsilon_2^{-\lambda k} \left\|\delta\mathbf{u}_{n+1}^f(k)\right\| &\le \|\mathbf{I} - \boldsymbol{\beta}\mathbf{Q}\mathbf{B}\mathbf{P}\| \cdot \sup_{k\in[0,K]} \varepsilon_2^{-\lambda k} \left\|\delta\mathbf{u}_n^f(k)\right\| \\ &\quad + \varepsilon_1 \|\mathbf{Q}\mathbf{B}\mathbf{P}\| \sup_{k\in[0,K]} \varepsilon_2^{-\lambda k} \sum_{j=0}^{k-1} \varepsilon_2^{k-j-1} \left\|\delta\mathbf{u}_n^f(j)\right\|.\end{aligned} \tag{A.16}$$

Since

$$\begin{aligned}&\sup_{k\in[0,K]} \varepsilon_2^{-\lambda k} \sum_{j=0}^{k-1} \varepsilon_2^{k-j-1} \left\|\delta\mathbf{u}_n^f(j)\right\| \\ &= \varepsilon_2^{-1} \sup_{k\in[0,K]} \left(\sum_{j=0}^{k-1} \varepsilon_2^{-\lambda j} \left\|\delta\mathbf{u}_n^f(j)\right\| \varepsilon_2^{(\lambda-1)(j-k)}\right) \\ &\le \varepsilon_2^{-1} \sup_{k\in[0,K]} \left(\sum_{j=0}^{k-1} \left(\sup_{k\in[0,K]} \varepsilon_2^{-\lambda j} \left\|\delta\mathbf{u}_n^f(j)\right\|\right) \varepsilon_2^{(\lambda-1)(j-k)}\right) \\ &\le \varepsilon_2^{-1} \left\|\delta\mathbf{u}_n^f(k)\right\|_\lambda \times \sup_{k\in[0,K]} \sum_{j=0}^{k-1} \varepsilon_2^{(\lambda-1)(j-k)} \\ &= \left\|\delta\mathbf{u}_n^f(k)\right\|_\lambda \times \frac{1 - \varepsilon_2^{-(\lambda-1)K}}{\varepsilon_2^\lambda - \varepsilon_2}\end{aligned} \tag{A.17}$$

then (A.16) becomes

$$\begin{aligned}\left\|\delta\mathbf{u}_{n+1}^f(k)\right\|_\lambda &\le \|\mathbf{I} - \boldsymbol{\beta}\mathbf{Q}\mathbf{B}\mathbf{P}\| \left\|\delta\mathbf{u}_n^f(k)\right\|_\lambda \\ &\quad + \varepsilon_1 \|\mathbf{Q}\mathbf{B}\mathbf{P}\| \left\|\delta\mathbf{u}_n^f(k)\right\|_\lambda \times \frac{1 - \varepsilon_2^{-(\lambda-1)K}}{\varepsilon_2^\lambda - \varepsilon_2}.\end{aligned} \tag{A.18}$$

Thus, there exists a sufficient large constant λ such that the following inequality holds when $\|\mathbf{I} - \boldsymbol{\beta}\mathbf{Q}\mathbf{B}\mathbf{P}\| < 1$, i.e.,

$$\|\mathbf{I} - \boldsymbol{\beta}\mathbf{Q}\mathbf{B}\mathbf{P}\| + \varepsilon_1 \|\mathbf{Q}\mathbf{B}\mathbf{P}\| \times \frac{1 - \varepsilon_2^{-(\lambda-1)K}}{\varepsilon_2^\lambda - \varepsilon_2} \le \rho < 1. \tag{A.19}$$

We can conclude that

$$\left\|\delta\mathbf{u}_{n+1}^f(k)\right\|_\lambda \le \rho \left\|\delta\mathbf{u}_n^f(k)\right\|_\lambda. \tag{A.20}$$

Equation (A.20) implies that $\lim_{n\to\infty} \|\delta\mathbf{u}_{n+1}^f(k)\|_\lambda = 0$, that is

$$\mathbf{u}_n^f(k) \to \mathbf{u}_d(k) \qquad \forall k \in [0, K].$$

To prove the convergence of the density, following the preceding derivation procedure, we obtain, from (A.14), that

$$\begin{aligned}&\left(\left\|\mathbf{u}_n^b(k-1)\right\|_\lambda + \left\|\Re\left(\delta\mathbf{x}_n(k)\right)\right\|_\lambda + \left\|\Re\mathbf{e}_n(k)\right\|_\lambda\right)\\&\quad\le \sup_{k\in[0,K]} \varepsilon_2^{-\lambda k}\sum_{j=0}^{k-1}\varepsilon_2^{k-j-1}\left\|\mathbf{QBP}\right\|\left\|\delta\mathbf{u}_n^f(j)\right\|\\&\quad= \left\|\mathbf{QBP}\right\|\left\|\delta\mathbf{u}_n^f(k)\right\|_\lambda \times \frac{1-\varepsilon_2^{-(\lambda-1)K}}{\varepsilon_2^\lambda-\varepsilon_2}. \qquad \text{(A.21)}\end{aligned}$$

Since the right-hand side of the equation tends to zero as the iteration goes infinity, and all the items on the left-hand side are nonnegative, so we can reach the final conclusion, i.e.,

$$\lim_{n\to\infty}\left\|\Re\left(\mathbf{y}_d(k)-\mathbf{y}_n(k)\right)\right\|_\lambda = 0.$$

■

APPENDIX B
PROOF OF THEOREM 4

The traffic system with input constraints becomes

$$\mathbf{x}_n(k+1) = f\left(\mathbf{x}_n(k),\mathbf{y}_n(k)\right) \qquad \text{(B.1)}$$

$$\begin{aligned}\mathbf{y}_n(k+1) =& \mathbf{A}\left(\mathbf{x}_n(k)\right)\mathbf{y}_n(k) + \mathbf{BP}sat\left(\mathbf{u}_n(k)\right)\\&+\boldsymbol{\eta}\left(\mathbf{x}_n(k)\right) - \mathbf{B}\cdot\mathbf{s}(k). \qquad \text{(B.2)}\end{aligned}$$

Define

$$\begin{aligned}\delta\mathbf{u}_{n+1}^f(k) =& \mathbf{u}_d(k) - \mathbf{u}_{n+1}^f(k)\\=& \mathbf{u}_d(k) - sat\left(\mathbf{u}_n(k)\right) - \boldsymbol{\beta}\Re\mathbf{e}_n(k+1). \qquad \text{(B.3)}\end{aligned}$$

Using (17) and Assumption 3, we have

$$\begin{aligned}&\Re\mathbf{e}_n(k+1)\\&\quad= \Re\{\mathbf{A}\left(\mathbf{x}_d(k)\right)\mathbf{y}_d(k) + \mathbf{BP}\mathbf{u}_d(k)\\&\qquad+\boldsymbol{\eta}\left(\mathbf{x}_d(k)\right) - \mathbf{B}\cdot\mathbf{s}(k) - \mathbf{A}\left(\mathbf{x}_n(k)\right)\mathbf{y}_n(k)\\&\qquad-\mathbf{BP}sat\left(\mathbf{u}_n(k)\right) - \boldsymbol{\eta}\left(\mathbf{x}_n(k)\right) + \mathbf{B}\cdot\mathbf{s}(k)\}\\&\quad= \Re\{\mathbf{A}\left(\mathbf{x}_d(k)\right)\mathbf{y}_d(k) - \mathbf{A}\left(\mathbf{x}_n(k)\right)\mathbf{y}_d(k)\\&\qquad+\mathbf{A}\left(\mathbf{x}_n(k)\right)\mathbf{y}_d(k) - \mathbf{A}\left(\mathbf{x}_n(k)\right)\mathbf{y}_n(k)\\&\qquad+\mathbf{BP}\mathbf{u}_d(k) + \boldsymbol{\eta}\left(\mathbf{x}_d(k)\right)\\&\qquad-\mathbf{BP}sat\left(\mathbf{u}_n(k)\right) - \boldsymbol{\eta}\left(\mathbf{x}_n(k)\right)\}\\&\quad= \Re\{\delta\mathbf{A}\left(\mathbf{x}_n(k)\right)\mathbf{y}_d(k) + \mathbf{A}\left(\mathbf{x}_n(k)\right)\mathbf{e}_n(k)\\&\qquad+\mathbf{BP}\left[\mathbf{u}_d(k) - sat\left(\mathbf{u}_n(k)\right)\right] + \delta\boldsymbol{\eta}\left(\mathbf{x}_n(k)\right)\}\\&\quad= \Re\left[\delta\mathbf{A}\left(\mathbf{x}_n(k)\right)\mathbf{y}_d(k)\right] + \Re\left[\mathbf{A}\left(\mathbf{x}_n(k)\right)\mathbf{e}_n(k)\right]\\&\qquad+\mathbf{QBP}\left[\mathbf{u}_d(k) - sat\left(\mathbf{u}_n(k)\right)\right] + \Re\left[\delta\boldsymbol{\eta}\left(\mathbf{x}_n(k)\right)\right].\end{aligned} \qquad \text{(B.4)}$$

Substituting (B.4) into (B.3) yields

$$\begin{aligned}\delta\mathbf{u}_{n+1}^f(k) =& \mathbf{u}_d(k) - sat\left(\mathbf{u}_n(k)\right) - \boldsymbol{\beta}\Re\mathbf{e}_n(k+1)\\=& \mathbf{u}_d(k) - sat\left(\mathbf{u}_n(k)\right)\\&-\boldsymbol{\beta}\{\Re[\delta\mathbf{A}(\mathbf{x}_n(k))\,\mathbf{y}_d(k)] + \Re[\mathbf{A}(\mathbf{x}_n(k))\mathbf{e}_n(k)]\\&+\mathbf{QBP}\left[\mathbf{u}_d(k) - sat\left(\mathbf{u}_n(k)\right)\right] + \Re[\delta\boldsymbol{\eta}\left(\mathbf{x}_n(k)\right)]\}\\=& \left(\mathbf{I}-\boldsymbol{\beta}\mathbf{QBP}\right)\left[\mathbf{u}_d(k) - sat\left(\mathbf{u}_n(k)\right)\right]\\&-\boldsymbol{\beta}\Re[\delta\mathbf{A}(\mathbf{x}_n(k))\,\mathbf{y}_d(k)] - \boldsymbol{\beta}\Re[\mathbf{A}(\mathbf{x}_n(k))\mathbf{e}_n(k)]\\&-\boldsymbol{\beta}\Re[\delta\boldsymbol{\eta}\left(\mathbf{x}_n(k)\right)]. \qquad \text{(B.5)}\end{aligned}$$

Note that

$$\begin{aligned}\delta\mathbf{u}_n(k) =& \mathbf{u}_d(k) - \mathbf{u}_n(k) = \mathbf{u}_d(k) - \mathbf{u}_n^f(k) - \mathbf{u}_n^b(k)\\=& \delta\mathbf{u}_n^f(k) - \mathbf{u}_n^b(k) \qquad \text{(B.6)}\end{aligned}$$

$$\left\|\mathbf{u}_n^b(k)\right\| \le \left\|\mathbf{u}_n^b(k-1)\right\| + \left\|\boldsymbol{\varphi}\right\|\left\|\Re\mathbf{e}_n(k)\right\|. \qquad \text{(B.7)}$$

Then, taking the norm on both sides of (B.5) and using Lemma 1, we have

$$\begin{aligned}&\left\|\delta\mathbf{u}_{n+1}^f(k)\right\|\\&\quad\le \left\|\mathbf{I}-\boldsymbol{\beta}\mathbf{QBP}\right\|\left\|\mathbf{u}_d(k) - sat\left(\mathbf{u}_n(k)\right)\right\|\\&\qquad+\left\|\boldsymbol{\beta}\right\|k_A b_{yd}\left\|\Re\left(\delta\mathbf{x}_n(k)\right)\right\|\\&\qquad+\left\|\boldsymbol{\beta}\right\|b_A\left\|\Re\mathbf{e}_n(k)\right\| + \left\|\boldsymbol{\beta}\right\|k_\eta\left\|\Re\left(\delta\mathbf{x}_n(k)\right)\right\|\\&\quad\le \left\|\mathbf{I}-\boldsymbol{\beta}\mathbf{QBP}\right\|\left\|\delta\mathbf{u}_n(k)\right\| + \left\|\boldsymbol{\beta}\right\|k_A b_{yd}\left\|\Re\left(\delta\mathbf{x}_n(k)\right)\right\|\\&\qquad+\left\|\boldsymbol{\beta}\right\|b_A\left\|\Re\mathbf{e}_n(k)\right\| + \left\|\boldsymbol{\beta}\right\|k_\eta\left\|\Re\left(\delta\mathbf{x}_n(k)\right)\right\|\\&\quad\le \left\|\mathbf{I}-\boldsymbol{\beta}\mathbf{QBP}\right\|\left\|\delta\mathbf{u}_n^f(k)\right\| + \left\|\mathbf{I}-\boldsymbol{\beta}\mathbf{QBP}\right\|\left\|\mathbf{u}_n^b(k-1)\right\|\\&\qquad+\left(\left\|\boldsymbol{\beta}\right\|k_A b_{yd} + \left\|\boldsymbol{\beta}\right\|k_\eta\right)\left\|\Re\left(\delta\mathbf{x}_n(k)\right)\right\|\\&\qquad+\left(\left\|\boldsymbol{\beta}\right\|b_A + \left\|\boldsymbol{\varphi}\right\|\left\|\mathbf{I}-\boldsymbol{\beta}\mathbf{QBP}\right\|\right)\left\|\Re\mathbf{e}_n(k)\right\|. \qquad \text{(B.8)}\end{aligned}$$

The relation (B.8) can be rewritten as

$$\begin{aligned}\left\|\delta\mathbf{u}_{n+1}^f(k)\right\| \le& \left\|\mathbf{I}-\boldsymbol{\beta}\mathbf{QBP}\right\|\cdot\left\|\delta\mathbf{u}_n^f(k)\right\|\\&+\varepsilon_1\left(\left\|\mathbf{u}_n^b(k-1)\right\| + \left\|\Re\left(\delta\mathbf{x}_n(k)\right)\right\| + \left\|\Re\mathbf{e}_n(k)\right\|\right)\end{aligned}$$

which is the same as (A.9). Therefore, by following the derivation procedure of Theorem 2, we can prove Theorem 4 in the same way. ■

REFERENCES

[1] M. Papageorgiou and A. Kotsialos, "Freeway ramp metering: An overview," *IEEE Trans. Intell. Transp. Syst.*, vol. 3, no. 4, pp. 271–281, Dec. 2002.

[2] M. Papageorgiou, H. Hadj-Salem, and F. Middleham, "ALINEA local ramp metering: Summary of the field results," *Transp Res. Rec. 1603*, TRB, Nat. Res. Council, Washington, DC, pp. 90–98, 1997.

[3] D. P. Masher, *Guidelines for Design and Operation of Ramp Control Systems*. Menlo Park, CA: Stanford Res. Inst., 1975.

[4] M. Papageorgiou, H. Hadj-Salem, and J. M. Blosseville, "ALINEA: A local feedback control law for on-ramp metering," *Transp Res. Rec. 1320*, pp. 58–64, 1991.

[5] E. Smaragdis, M. Papageorgiou, and E. Kosmatopoulos, "A flow-maximizing adaptive local ramp metering strategy," *Transp. Res. B*, vol. 38, no. 3, pp. 251–270, Mar. 2004.

[6] L. L. Chen, A. D. May, and D. M. Auslander, "Freeway ramp control using fuzzy set theory for inexact reasoning," *Transp. Res. A*, vol. 24, no. 1, pp. 15–25, Jan. 1990.

[7] H. M. Zhang and S. G. Ritchie, "Freeway ramp metering using artificial neural networks," *Transp. Res. C*, vol. 5, no. 5, pp. 273–286, Oct. 1997.

[8] Z. S. Hou, J. X. Xu, and H. W. Zhong, "Freeway traffic control using iterative learning control-based ramp metering and speed signaling," *IEEE Trans. Veh. Technol.*, vol. 56, no. 2, pp. 466–477, Mar. 2007.
[9] Z. S. Hou, J. X. Xu, and J. W. Yan, "An iterative learning approach for density control of freeway traffic flow via ramp metering," *Transport. Res. C*, vol. 16, no. 1, pp. 71–97, Feb. 2008.
[10] S. Arimoto, S. Kawamura, and F. Miyazaki, "Bettering operation of robots by learning," *J. Robot. Syst.*, vol. 1, no. 2, pp. 123–140, 1984.
[11] J.-X. Xu, Y. Tan, and T.-H. Lee, "Iterative learning control design based on composite energy function with input saturation," *Automatica*, vol. 40, no. 8, pp. 1371–1377, Aug. 2004.
[12] C. J. Chien, "A discrete iterative learning control for a class of nonlinear time-varying systems," *IEEE Trans. Automat. Control*, vol. 43, no. 5, pp. 748–752, May 1998.
[13] Y. Q. Chen and C. Y. Wen, "Iterative Learning Control: Convergence, Robustness and Applications," in *Lecture Notes in Control and Information Sciences*. New York: Springer-Verlag, 1999.
[14] M. J. Lighthill and G. B. Whitham, "On the kinematic waves II: A theory of traffic flow on long crowded roads," *Proc. R. Soc. Lond. A, Math. Phys. Sci.*, vol. 229, no. 1178, pp. 317–345, May 1955.
[15] H. J. Payne, "Models of freeway traffic and control," in *Proc. Math. Models Public Syst., Simul. Council*, 1971, pp. 51–61.
[16] H. J. Payne, "A critical review of a macroscopic freeway model," in *Proc. Eng. Found. Conf. Res. Directions Comput. Control Urban Traffic Syst.*, 1979, pp. 251–265.
[17] M. Parageorgiou, J. M. Blosseville, and H. Hadj-Salem, "Macroscopic modeling of traffic flow on the Boulevard Peripherique in Paris," *Transp. Res. B*, vol. 23, no. 1, pp. 29–47, Feb. 1989.
[18] M. Parageorgiou, J. M. Blosseville, and H. Hadj-Salem, "Modeling and real time control on traffic flow on the southern part of Boulevard Peripherique in Paris. Part I: Modeling," *Transp. Res. A*, vol. 24, no. 5, pp. 345–359, Sep. 1990.
[19] M. Parageorgiou, J. M. Blosseville, and H. Hadj-Salem, "Modeling and real time control on traffic flow on the southern part of Boulevard Peripherique in Paris. Part II: Coordinated on-ramp metering," *Transp. Res. A*, vol. 24, no. 5, pp. 361–370, Sep. 1990.
[20] M. X. Sun and D. Wang, "Initial shift issues on discrete-time iterative learning control with system relative degree," *IEEE Trans. Automat. Control*, vol. 48, no. 1, pp. 144–148, Jan. 2003.

Zhongsheng Hou received the B.S. and M.S. degrees in applied mathematics from Jilin University of Technology, Changchun, China, in 1983 and 1988, respectively, and the Ph.D. degree in control theory from Northeastern University, Shenyang, China, in 1994.

He was a Postdoctoral Fellow with the Harbin Institute of Technology, Harbin, China, from 1995 to 1997 and a Visiting Scholar with Yale University, New Haven, CT, from 2002 to 2003. In 1997, he joined the Beijing Jiaotong University, Beijing, China, where he is currently a Full Professor and the Head of the Department of Automatic Control. He has about 80 peer-reviewed journal papers published and 100 papers in prestigious conference proceedings. He is the author of the monograph *Nonparametric Model and Its Adaptive Control Theory* (Science Press of China) and the holder of the patent invention *Model Free Control Technique* (Chinese Patent ZL 94 1 12504. 1, issued in 2000). His research interests are in the fields of data-driven control, model-free adaptive control, learning control, and intelligent transportation systems.

Xin Xu was born in Hubei, China, in 1974. He received the B.S. degree in control engineering in 1996 and the Ph.D. degree in electrical engineering from the National University of Defense Technology (NUDT), Changsha, China.

From 2003 to 2004, he was a Postdoctoral Fellow with the School of Computers, NUDT. He is currently a Professor with the Institute of Automation, College of Mechantronics and Automation, NUDT. He has coauthored four books and published more than 40 papers in international journals and conferences. His research interests include reinforcement learning, data mining, and learning control.

Jingwen Yan received the B.S., M.S., and Ph.D. degrees from Beijing Jiaotong University, Beijing, China, in 2004, 2006, and 2009, respectively.

She is currently with the Advanced Control Systems Laboratory, School of Electronic and Information Engineering, Beijing Jiaotong University. Her research interests are in fields of iterative learning control and traffic control.

Jian-Xin Xu (M'92–SM'98) received the B.S. degree in electrical engineering from Zhejiang University, Hangzhou, China, in 1982 and the M.S. and Ph.D. degrees in electrical engineering from the University of Tokyo, Tokyo, Japan, in 1986 and 1989, respectively.

He worked for one year with Hitachi Research Laboratory, Japan, and for more than one year with The Ohio State University, Columbus, as a Visiting Scholar. Since 1991, he has been with the National University of Singapore, Singapore, where he is currently a Full Professor with the Department of Electrical and Computer engineering. He has 90 peer-reviewed papers published or to appear, ten chapters in edited books, and 160 papers in prestigious conference proceedings. He coauthored a book *Linear and Nonlinear Iterative Learning Control* (Springer-Verlag, 2003). He is an Associate Editor of the *Asian Journal of Control*. His research interests lie in the fields of learning control, variable structure control, fuzzy logic control, discontinuous signal processing, and applications to motion control and process control problems.

Dr. Xu is a member of the technical committee on variable structure systems and sliding mode control of the IEEE Control Systems Society.

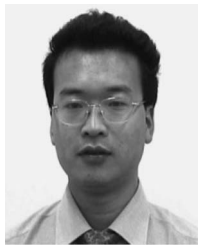

Gang Xiong was born in 1969. He received the B.S. and M.S. degrees from Xi'an University of Science and Technology, Xi'an, China, in 1991 and 1994, respectively, and the Ph.D. degrees in control science and engineering from Shanghai Jiao Tong University, Shanghai, China, in 1996.

From 1996 to 1998, he was a Postdoctoral Researcher with Zhejiang University, Hangzhou, China. From 1998 to 2001, he was a Senior Research Fellow with Tampere University of Technology, Tampere, Finland. From 2001 to 2007, he was a Specialist with Nokia Corporation, Finland. In 2007, he was a Senior Consultant with Accenture and Chevron. In 2008, he was a Deputy Director with Informatization Office, Chinese Academy of Science (CAS), Beijing, China. In 2009, he started his current work as Deputy Director of the Parallel Control and Management Center, a Research Scientist with the Automation Institute, CAS. He is the author or coauthor of about 100 refereed journal and conference papers. His research interests include parallel control and management, modeling and optimization of complex systems, intelligent transportation systems, intelligent manufacturing, and smart grid.